Disulfide isomerization switches tissue factor from coagulation to cell signaling

Jasimuddin Ahamed*†, Henri H. Versteeg*†, Marjolein Kerver*, Vivien M. Chen‡, Barbara M. Mueller§, Philip J. Hogg‡, and Wolfram Ruf*¶

*Department of Immunology, The Scripps Research Institute, SP258, 10550 North Torrey Pines Road, La Jolla, CA 92037; ‡Centre for Vascular Research, University of New South Wales, Sydney 2052, Australia; and §La Jolla Institute for Molecular Medicine, San Diego, CA 92121

Communicated by Earl W. Davie, University of Washington, Seattle, WA, July 27, 2006 (received for review June 7, 2006)

Cell-surface tissue factor (TF) binds the serine protease factor VIIa to activate coagulation or, alternatively, to trigger signaling through the G protein-coupled, protease-activated receptor 2 (PAR2) relevant to inflammation and angiogenesis. Here we demonstrate that TF·VIIa-mediated coagulation and cell signaling involve distinct cellular pools of TF. The surface-accessible, extracellular Cys^{186}–Cys^{209} disulfide bond of TF is critical for coagulation, and protein disulfide isomerase (PDI) disables coagulation by targeting this disulfide. A TF mutant (TF C209A) with an unpaired Cys^{186} retains TF·VIIa signaling activity, and it has reduced affinity for VIIa, a characteristic of signaling TF on cells with constitutive TF expression. We further show that PDI suppresses TF coagulant activity in a nitric oxide-dependent pathway, linking the regulation of TF thrombogenicity to oxidative stress in the vasculature. Furthermore, a unique monoclonal antibody recognizes only the noncoagulant, cryptic conformation of TF. This antibody inhibits formation of the TF·PAR2 complex and TF·VIIa signaling, but it does not prevent coagulation activation. These experiments delineate an upstream regulatory mechanism that controls TF function, and they provide initial evidence that TF·VIIa signaling can be specifically inhibited with minimal effects on coagulation.

allosteric disulfide | protein disulfide | isomerase | S-nitrosylation | G protein-coupled receptor

Coagulation activation and platelet deposition are increasingly recognized as important events in inflammation, cancer, and angiogenesis. Tissue factor (TF), a member of the cytokine receptor family, binds and allosterically activates factor VIIa. The enzymatic TF·VIIa complex then recruits substrate factor X in the ternary TF·VIIa·X coagulation-initiation complex (1) to generate Xa and ultimately thrombin required for physiological hemostasis (2). The TF·VIIa complex also directly cleaves protease-activated receptor 2 (PAR2) (3, 4) and thus contributes to nonhemostatic roles of the TF pathway in cancer and inflammation (5, 6). Although PAR2 has been identified as the target for a number of proteases (7), the link between TF and PAR2 appears to be close. The TF cytoplasmic domain is specifically phosphorylated downstream of PAR2 signaling (8), and TF cytoplasmic domain-deleted mice display a proangiogenic phenotype dependent on PAR2 (9).

Fundamentally, it was not clear how the concomitant coagulation activation and thrombin generation would allow for physiologically meaningful direct signaling by the TF·VIIa complex. TF is known to be present in a noncoagulant or "cryptic" form on the cell surface, but whether the noncoagulant pool is involved in TF·VIIa signaling is unknown (10). In part, cryptic TF is sequestered from lipids that support coagulation reactions, but the absence of procoagulant lipids cannot entirely account for the significantly reduced affinity of TF for VIIa that is documented in cell-signaling experiments (11). Therefore, TF may have alternative conformations with distinct functional properties. Here, we provide insight into these open questions by identifying disulfide exchange mediated by extracellular protein disulfide isomerase (PDI) as a regulatory mechanism that switches TF between coagulation and TF·VIIa signaling. We further describe a monoclonal antibody that binds to the noncoagulant conformation and inhibits TF·VIIa signaling by preventing formation of the TF·PAR2 complex. Thus, it is feasible to block TF·VIIa signaling without compromising TF-dependent hemostasis.

Results

Different Cellular Pools of TF Mediate Coagulation Activation and TF·VIIa Signaling. To address the regulation of TF functions in coagulation and signaling, we focused on a cell model with constitutive TF expression. We found that the coagulant activity of TF remained unchanged despite progressive loss of TF expression to <5% in human HaCaT keratinocytes during growth arrest (Fig. 1*A*). A set of antibodies for distinct epitopes was used to evaluate TF expression on the cell surface. mAb 9C3 binds close to the VIIa-binding site, whereas mAb 5G9 inhibits coagulation by competing with substrate factor X binding (12, 13). mAb 10H10 and mAb 5G9 do not inhibit VIIa binding, and they bind to partially overlapping epitopes, but mAb 10H10 does not block coagulation activation. Staining of nonpermeabilized cells with mAb 9C3 or 5G9 (Fig. 1*B*) or surface biotinylation (data not shown) indicated that cell-surface expression, rather than intracellular pools of TF, changed during growth arrest. Inhibition of coagulation by mAb 5G9 was independent of time of culture (Fig. 1*C*). Unexpectedly, mAb 10H10 lost reactivity with the remaining coagulant pool of TF at day 5 (Fig. 1*B*). Furthermore, immobilized mAb 10H10 depleted <20% and mAb 5G9 >85% of the coagulant activity from a preparation of phospholipid-reconstituted, purified TF (Fig. 1*D*). Taken together, these data indicate that mAb 10H10 has low affinity for the minor cellular pool of coagulant TF but recognizes cryptic pools of TF.

Unlike coagulant activity, TF·VIIa signaling gradually decreased from day 1 to day 6 (Fig. 1*E*). TF·VIIa signaling on these cells was PAR2-dependent, but PAR2 activation with the direct agonist SLIGRL or thrombin signaling was unchanged during prolonged culture (Fig. 1*F*). Cell-surface-expressed TF binds VIIa with variable affinity (14), and TF-dependent Xa generation is saturated at lower VIIa concentrations relative to TF·VIIa signaling (15). Irrespective of time of culture, coagulant TF on cells had high affinity for VIIa because rates of Xa generation were saturated to ≈99% at 1 nM VIIa. Only high (10 nM) but not low (1 nM) concentrations of VIIa induced signaling by the binary TF·VIIa complex on cells at day 1 (Fig. 1*G*), and the addition of a potent Xa inhibitor (NAP5) excluded signaling by

Conflict of interest statement: No conflicts declared.

Abbreviations: GSH, glutathione; GSNO, *S*-nitrosoglutathione; HUVEC, human umbilical vein endothelial cell; MPB, N^{α}-(3-maleimidylpropionyl)biocytin; NAP5, nematode anticoagulant protein 5; PAO, phenylarsine oxide; PAR2, protease-activated receptor 2; PDI, protein disulfide isomerase; SNP, sodium nitroprusside; TF, tissue factor.

†J.A. and H.H.V. contributed equally to this work.

¶To whom correspondence should be addressed. E-mail: ruf@scripps.edu.

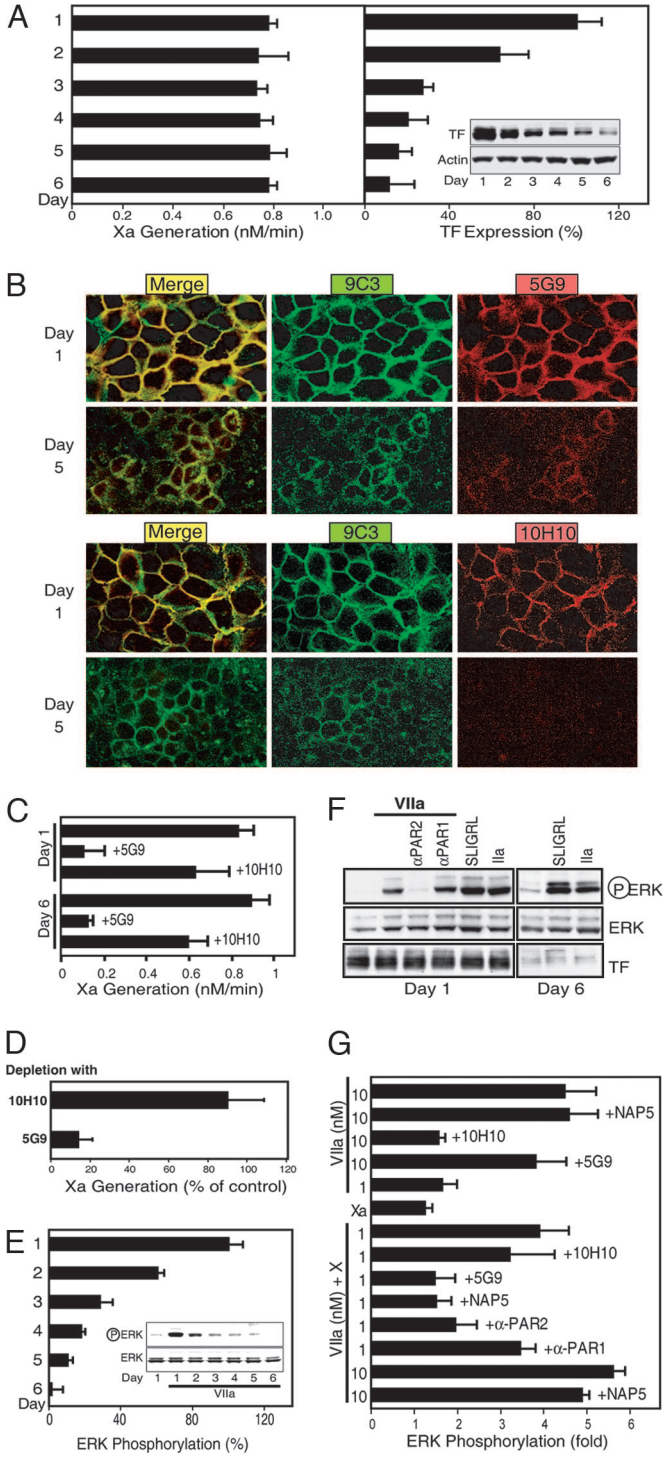

Fig. 1. TF·VIIa signaling and coagulation initiation are mediated by distinct cell-surface pools of TF. (*A*) TF coagulant activity measured as Xa generation and TF expression quantified from Western blots during growth arrest of HaCaT cells. Results are expressed as the mean ± SD ($n = 3$). (*Insets*) Representative Western blots for actin or TF in cell lysates. (*B*) Detection of cell-surface TF with FITC-conjugated mAb 9C3 and Texas red-conjugated mAb 5G9 or 10H10 by confocal microscopy. (*C*) mAb 5G9 but not mAb 10H10 inhibits TF coagulant activity equally during growth arrest. (*D*) Immobilized mAb 5G9 but not mAb 10H10 immunodepletes coagulation activity from preparations of phospholipid-reconstituted TF. (*E*) TF·VIIa signaling is down-regulated during growth arrest. (*Insets*) Representative Western blots for phosphorylated and nonphosphorylated ERK after 10 min of stimulation. (*F*) PAR2 agonist SLIGRL and thrombin responses are not down-regulated during growth arrest. Pretreatment of cells at day 1 with inhibitory antibodies to PAR1 or PAR2 shows PAR2 dependence of TF·VIIa signaling. (*G*) mAb 10H10 specifically inhibits TF·VIIa signaling. Different affinity for VIIa distinguishes TF that mediates TF·VIIa or ternary TF·VIIa·Xa complex signaling. At 1 nM VIIa, cells display only Xa-dependent TF·VIIa·Xa signaling that is inhibited by the specific Xa inhibitor nematode anticoagulant protein 5 (NAP5) or mAb 5G9. At 10 nM VIIa, direct signaling of TF·VIIa occurs that is not inhibited by NAP5 or mAb 5G9 but is blocked by mAb 10H10. ERK phosphorylation at 10 min was quantified (mean ± SD; $n > 3$).

other downstream coagulation factors. Importantly, mAb 10H10, with poor reactivity toward coagulant TF, efficiently blocked TF·VIIa signaling. Although mAb 5G9 was reactive with coagulant and noncoagulant pools of TF on cells (Fig. 1 *A* and *B*), TF·VIIa signaling was not inhibited by this antibody.

In addition to direct cleavage of PAR2 by the TF·VIIa complex, TF also serves as a scaffold to assemble the ternary TF·VIIa·X coagulation complex in which nascent product Xa signals by activating PARs (4). One nanomolar VIIa was sufficient for TF·VIIa·Xa signaling that was blocked by the Xa inhibitor NAP5 and by mAb 5G9, which blocks the substrate X-binding site on TF (Fig. 1*G*). mAb 10H10 did not block ternary TF·VIIa·Xa complex signaling, consistent with its poor affinity for coagulant TF. Thus, antigenically distinct pools of TF are responsible for coagulation activation versus TF·VIIa signaling, and the inhibitory profile of mAb 10H10 shows that TF·VIIa signaling can be blocked with minimal effects on coagulation.

Redox State of the TF Cys^{186}–Cys^{209} Disulfide Determines TF·VIIa Signaling Specificity. We reasoned that a conformational change in TF is responsible for differences in VIIa affinity, and we focused on the exposed TF Cys^{186}–Cys^{209} disulfide bond, which is required for coagulation activation (16). The Cys^{186}–Cys^{209} disulfide is solvent-exposed, and such cross-strand disulfides between parallel β-strands are less stable because of the strained bond geometry (17–19). Alanine substitution mutants for Cys^{186} or Cys^{209} were expressed by adenoviral transduction of human umbilical vein endothelial cells (HUVECs) to surface levels similar to wild-type TF, based on flow cytometry or mAb 9C3 staining (Fig. 2*A*). Each mutant showed >95% diminished TF·VIIa-mediated Xa generation. TF·VIIa signaling appeared normal with C209A, but no signaling was detectable with C186A TF (Fig. 2*B*). Dose–response curves showed that TF·VIIa signaling in wild-type TF-expressing cells required 1 nM VIIa or more, but TF·VIIa·Xa signaling was saturated at this concentration of VIIa (Fig. 2*C*). With C209A TF, TF·VIIa signaling required slightly lower concentrations of VIIa relative to wild-type TF, but C209A TF-mediated signaling did not change when substrate X was added. Thus, formation of the Cys^{186}–Cys^{209} disulfide is required to generate TF with high affinity for VIIa, full coagulant activity, and concomitant ternary TF·VIIa·Xa complex signaling.

Expression of soluble C209A TF yielded both monomers and dimers, but purified dimers were inactive in a chromogenic assay that measures the allosteric induction of VIIa catalytic activity. In contrast, monomeric soluble C209A TF activated VIIa, but with diminished affinity relative to wild-type TF (Fig. 2*D*). Thus, breaking of the Cys^{186}–Cys^{209} disulfide reduces affinity for VIIa; but at saturation, C209A TF fully activated VIIa, which is necessary for proteolytic cell signaling through PAR2. C209A appears to be prone to mixed disulfide formation, and surface biotinylation showed a large fraction of C209A TF in a cell-surface SDS-stable dimer (Fig. 2*E*). The molecular weight of the surface C209A TF dimer differed from that in intracellular pools, but after deglycosylation the mobility was similar (data not shown). Consistent with formation of a C209A TF homodimer on the cell surface, Western blotting of TF immunoprecipitates

BIOCHEMISTRY

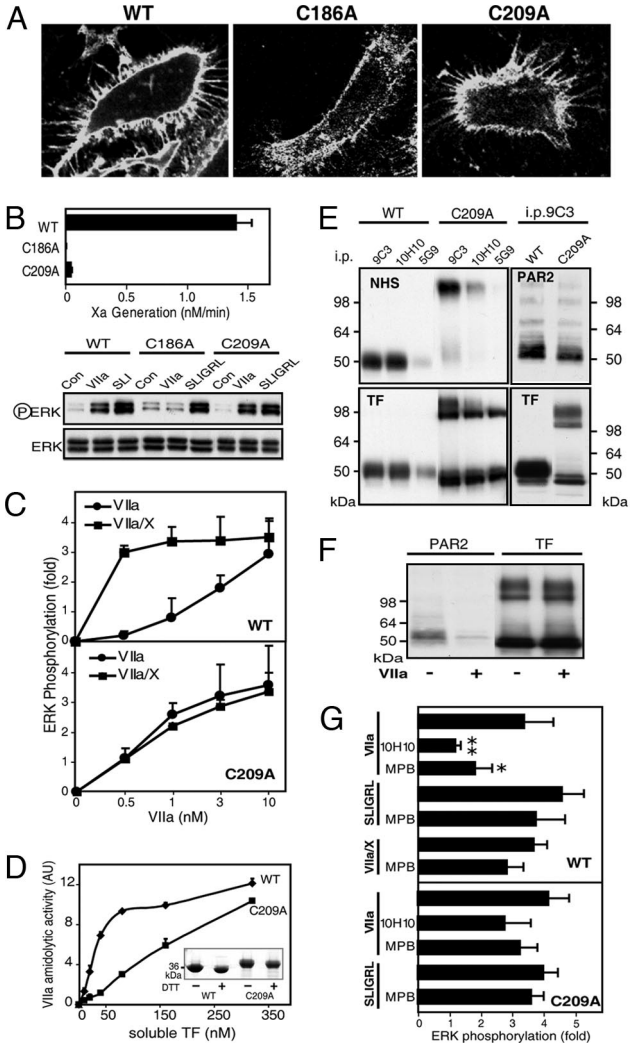

Fig. 2. The TF Cys^{186}–Cys^{209} disulfide controls TF signaling specificity. (*A*) Cell-surface expression shown by FITC-labeled mAb 9C3 staining of wild-type (WT), C186A, or C209A TF in HUVECs cotransduced with PAR2. (*B*) Mutation of Cys^{186} or Cys^{209} reduces coagulation, but only C209A TF retains TF·VIIa signaling activity. Control (Con) experiments (not shown) revealed no VIIa signaling in cells that were transduced only with PAR2 or vector control, excluding that adenovirus transduction induced the up-regulation of endogenous TF under these conditions. (*C*) Dose–response of VIIa signaling with and without 100 nM X in HUVECs expressing C209A or WT TF. ERK phosphorylation was quantified at 10 min (mean ± SD; $n > 4$). (*D*) Recombinant soluble C209A TF enhances catalytic activity of VIIa (40 nM) with reduced affinity relative to WT TF (mean ± SD; $n = 3$). AU, arbitrary units. (*Inset*) Gel of homogeneous preparations of monomeric soluble TF; the expression tag was not cleaved from C209A TF, yielding a higher molecular mass. (*E*) Cell-surface expression of WT and C209A TF determined by NHS surface biotinylation. mAb 5G9 epitope loss after surface NHS modification was used to demonstrate relative abundance of intra- and extracellular pools. The majority of cell-surface C209A TF was present as an SDS-stable homodimer with a consistently observed pool of C209A TF monomer in PAR2-transduced cells. PAR2 coimmunoprecipitated (i.p.) with WT or C209A TF in an SDS-labile complex. (*F*) PAR2 detection in mAb 9C3 immunoprecipitates of C209A TF is sensitive to pretreatment of cells with VIIa. (*G*) Inhibition of WT TF·VIIa signaling by thiol blockade. TF- and PAR2-transduced HUVECs were pretreated with 100 μM MPB or 50 μg/ml mAb 10H10 for 15 min before stimulation with 10 nM VIIa, 0.5 nM VIIa, and 100 nM X, or SLIGRL (mean ± SD; $n = 3$).

for PAR2 further excluded the formation of an SDS-stable heterodimer with PAR2 (Fig. 2*E*). Because the purified C209A dimer was inactive, we conclude that the small pool of monomeric, cell-surface-expressed C209A TF mediated cell signaling.

TF·VIIa signaling of wild-type or C209A TF-expressing cells required PAR2 cotransduction, and it was blocked by anti-PAR2 antibody. Although PAR2 and C209A TF did not form an SDS-stable complex, both mutant and wild-type TF similarly coimmunoprecipitated PAR2. The degree of PAR2 complex formation was consistent with the similar TF·VIIa signaling activity of C209A versus wild-type TF. Our PAR2 antibody recognizes the activation region of PAR2. Pretreatment of cells with VIIa for 10 min abolished PAR2 detection in C209A TF immunoprecipitates (Fig. 2*F*), indicating that the immunoprecipitated pool of PAR2 is cleaved on the cell surface and participates in cell signaling. Although wild-type TF was expressed at 50- to 100-fold higher cell-surface levels than monomeric C209A TF, TF·VIIa signaling was not different between mutant and wild-type TF in the depicted MAP kinase phosphorylation assay (Fig. 2*B*) or gene-induction readouts, such as TR3 up-regulation (20) (data not shown). We conclude from these findings that only a minor fraction of wild-type TF is present in a PAR2-signaling complex and that high cell-surface TF expression levels are not required for efficient TF·VIIa signaling.

mAb 10H10 had poor reactivity for surface pools of C209A TF, but it efficiently immunoprecipitated intracellular pools (Fig. 2*E*). Unlike wild-type TF·VIIa signaling, mAb 10H10 did not block C209A TF signaling (Fig. 2*G*), indicating that inhibition of signaling is through targeting of extracellular pools of TF. We hypothesized that dynamic disulfide/thiol exchange generated signaling-active wild-type TF, whereas the small surface pool of monomeric C209A TF was in a more stable, slowly exchanging linkage with PAR2. Pretreatment of cells with the relative membrane-impermeant thiol blocker N^{α}-(3-maleimidylpropionyl)biocytin (MPB) inhibited wild-type TF·VIIa but not C209A TF·VIIa signaling (Fig. 2*G*). Importantly, MPB pretreatment blocked neither direct PAR2 agonist responses nor signaling of the ternary wild-type TF·VIIa·Xa complex, which requires TF with an intact Cys^{186}–Cys^{209} disulfide. Thus, only TF·VIIa signaling is sensitive to extracellular thiol blockade.

Association of PDI with TF. To address cellular mechanisms by which the TF disulfide is broken, we established conditions that modulate TF function without changing constitutive expression of TF in HaCaT cells. Cells were seeded into Ca^{2+}-depleted medium to prevent cell–cell contacts for 48 h. Alternatively, medium was supplemented for the last 24 h with 2 mM Ca^{2+} (high Ca^{2+}), which induced distinct epithelial morphology as expected. mAb 9C3 immunoprecipitated equivalent amounts of surface-biotinylated TF under both conditions. Similar cell-surface expression and lack of significant intracellular pools were further confirmed by pulldown with mAb 5G9, which does not immunoprecipitate TF after cell-surface biotinylation (Fig. 3*A*). For functional assays, cells were equilibrated for 10 min in serum-free medium containing Ca^{2+} to support coagulation and signaling reactions. TF showed marked functional differences under the two culture conditions (Fig. 3*B*). Coagulant activity was ≈3- to 6-fold higher in low-Ca^{2+} cells, whereas TF·VIIa signaling was detectable only in high-, but not low-, Ca^{2+} cells. Direct PAR2 activation with agonist peptide was comparable under both conditions, excluding loss of PAR2 signaling. Thus, the cell-surface environment of high-Ca^{2+} cells favored TF signaling while disabling coagulation.

We hypothesized that a reductive PDI pathway targets the TF Cys^{186}–Cys^{209} disulfide bond to suppress coagulation. MPB-labeling yielded coprecipitating thiol-biotinylated bands of ≈56 and 64 kDa in mAb 9C3 pulldowns specifically from high-Ca^{2+} cells (Fig. 3*C*). Blocking vicinal thiols with PAO abolished labeling of these bands, but a faint labeled band at the appropriate molecular mass for TF became somewhat more prominent. Anti-PDI also precipitated MPB-labeled bands of 56 and

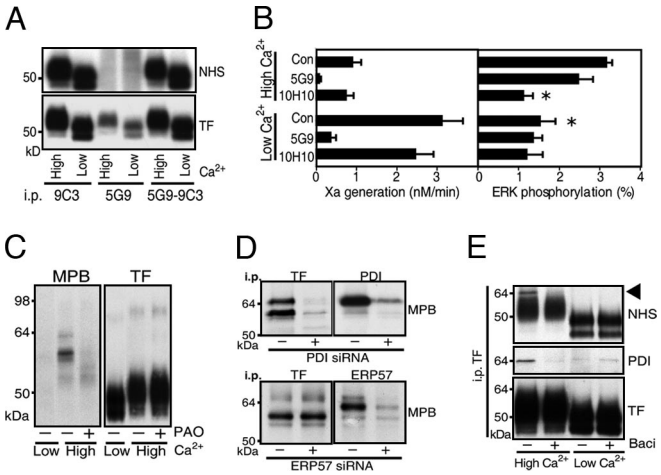

Fig. 3. Extracellular PDI is associated with TF. (*A*) A 24-h elevation of extracellular Ca^{2+} yields similar TF cell surface expression relative to HaCaT cells in low Ca^{2+}. TF was immunoprecipitated (i.p.) from NHS surface-biotinylated cells with mAb 9C3 or 5G9. mAb 5G9 does not bind biotinylated TF that is recovered in subsequent mAb 9C3 pulldown. (*B*) Low coagulant activity of TF in high-Ca^{2+} cells is associated with TF·VIIa signaling that is inhibited by mAb 10H10. *, Different from high-Ca^{2+} control ($P < 0.01$, *t* test; mean ± SD; $n > 4$). (*C*) MPB labeling of proteins coprecipitating with TF mAb 9C3 pulldown is inhibited by blockade of vicinal thiols by 2 μM phenylarsine oxide (PAO). (*D*) PDI but not ERP57 knockdown with siRNA prevents MPB-labeled bands in TF immunoprecipitates. (*E*) NHS surface-biotinylated PDI is specifically associated with high-Ca^{2+} cells. The PDI inhibitor bacitracin (3 mM) also dissociates PDI from TF in mAb 9C3 immunoprecipitates, but it has no effect on low-Ca^{2+} cells.

64 kDa (Fig. 3*D*), but the 56-kDa species was typically only a minor fraction in PDI immunoprecipitates. We considered whether the 56-kDa band was the close PDI homolog ERP57, but ERP57 knockdown with siRNA demonstrated that bands coprecipitating with TF were not ERP57, but instead they depended on high levels of PDI expression (Fig. 3*D*). Western blotting showed that PDI association with TF immunoprecipitates was increased in high- versus low-Ca^{2+} cells, and NHS surface biotinylation confirmed that PDI association with TF was extracellular (Fig. 3*E*). Thus, PDI is associated with TF on the cell surface when coagulant activity is low and TF·VIIa signaling is enabled.

PDI Regulates TF Coagulant Activity Through NO-Dependent Pathways. Brief exposure of cells to the oxidizing agent Hg^{2+} dissociated MPB-labeled PDI from TF, and it also abolished staining with cryptic TF-specific mAb 10H10. TF cell-surface expression based on mAb 9C3 staining (Fig. 4*A*) or surface biotinylation (data not shown) did not change. Exposure to Hg^{2+} further restored coagulant activity of high-Ca^{2+} cells to levels that were comparable to low-Ca^{2+} cells (Fig. 4*B*). Hg^{2+} had minimal effects on TF coagulant activity of low-Ca^{2+} cells, indicating that Hg^{2+} did not increase procoagulant phospholipids under the experimental conditions. Thiol blockade with 50 mM methyl methanethiolsulfonate (MMTS) did not change baseline TF activity, but it did reduce the Hg^{2+} effect on TF activity from 5- to 6-fold to <2-fold. MMTS blocked free thiols of surface PDI, indicating that PDI is required for the activating effect of Hg^{2+}. PDI expression was reduced by siRNA to 32 ± 13% of control levels, based on Western blotting. Decreased PDI expression was associated with an ≈2-fold increase of TF coagulant activity (Fig. 4*B*). Importantly, after Hg^{2+} activation, TF procoagulant activity was similar in siRNA-treated cells and controls. These data provide additional evidence that Hg^{2+} selectively reversed PDI-mediated suppression of TF procoagulant function.

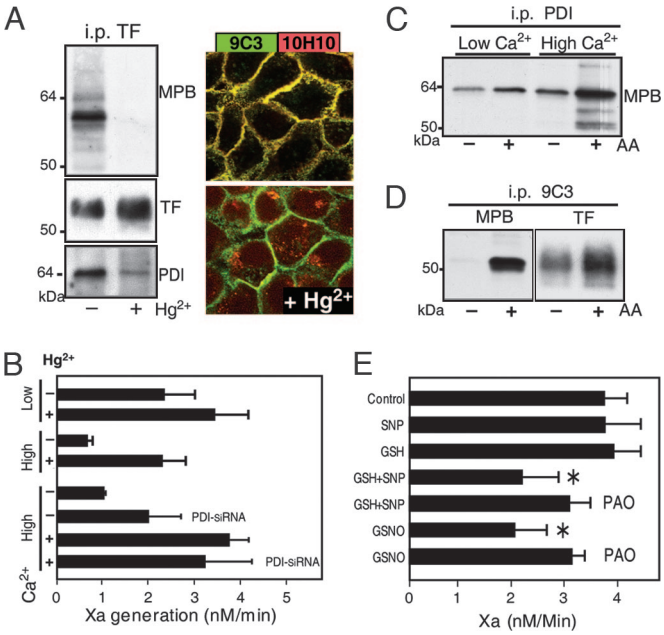

Fig. 4. NO-dependent suppression of TF coagulant activity by PDI. (*A*) A 2-min exposure to 100 μM Hg^{2+} dissociates MPB-labeled PDI from anti-TF mAb 9C3 immunoprecipitates (i.p.) and abolishes mAb 10H10 staining of TF. (*B*) Hg^{2+} treatment induces coagulation specifically on high-Ca^{2+} cells. Knockdown of PDI in high-Ca^{2+} cells increases TF coagulant activity without changing maximal function after Hg^{2+} treatment. (*C*) The biotin-switch method after thiol blockade with 1 mM *N*-ethylmaleimide detects increased labeling of PDI after NO release by ascorbic acid (AA) specifically in PDI immunoprecipitates from high-Ca^{2+} cells. (*D*) S-nitrosylation of TF detected by the biotin-switch method after thiol blockade with 1 mM iodoacetamide before MPB-labeling with or without ascorbic acid. (*E*) Hg^{2+}-induced activation of TF coagulant activity is reversible by NO-dependent PDI pathways. Cells washed after brief 100 μM Hg^{2+} exposure were incubated in Hepes buffer, pH 7.4/1.5 mM Ca^{2+} in the presence of 1 mM SNP, 1 mM reduced glutathione (GSH), or 1 mM *S*-nitrosoglutathione (GSNO) with or without 10 μM PAO for 10 min before the Xa generation assay. *, Different from control ($P < 0.05$, *t* test; mean ± SD; $n = 3$).

The mutational analysis showed that breaking the Cys^{186}–Cys^{209} disulfide renders TF coagulation inactive, but MPB labeling showed no prominent free thiols of TF on high-Ca^{2+} cells. Cell-surface PDI catalyzes transnitrosylation and denitrosylation reactions (21, 22), and PDI can be S-nitrosylated at vicinal thiols (23). Fifty to 100 μM Hg^{2+} was required to enhance TF coagulant activity, which is typical of the concentrations needed to release nitric oxide (NO) from PDI (23), raising the possibility that the activating effect of Hg^{2+} involved denitrosylation of PDI. The biotin-switch method (24) was used to detect S-nitrosylation. After blocking cellular free thiols with *N*-ethylmaleimide, cells were MPB-labeled in the presence or absence of ascorbic acid to release NO. With specificity for high-Ca^{2+}cells, immunoprecipitated PDI showed increased MPB labeling in the presence of ascorbic acid (Fig. 4*C*). MPB-labeled bands at the appropriate molecular mass for TF also became visible in PDI immunoprecipitates. Similarly, after blockade of free thiols with 1 mM iodoacetamide, MPB labeling of TF immunoprecipitates significantly increased in the presence of ascorbic acid (Fig. 4*D*). These data indicated that inactivation of TF coagulant activity depends on NO.

We tested whether Hg^{2+}-induced activation of TF was reversible. After washout of the oxidant, coagulant activity of TF remained high. The addition of reduced GSH or the NO donor SNP alone had no effect on TF activity, but in combination TF coagulant activity was suppressed (Fig. 4*E*). The vicinal thiol

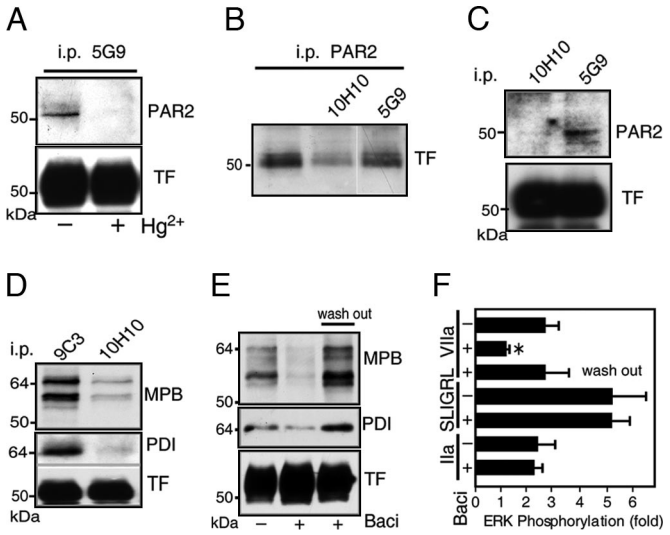

Fig. 5. TF·PAR2 complex formation is required for TF·VIIa signaling. (*A*) mAb 5G9 immunoprecipitation (i.p.) of PAR2 from high-Ca^{2+} cells is abolished by Hg^{2+} pretreatment. (*B*) mAb 10H10 but not mAb 5G9 perturbs the TF·PAR2 complex. HaCaT cells were pretreated in serum-free medium for 15 min with the indicated antibody, and TF was detected in the PAR2 immunoprecipitate. Loading controls were not feasible due to background because no PAR2-suitable antibody from a different species was available for Western blotting. (*C*) mAb 10H10 does not immunoprecipitate PAR2 from HaCaT cells. (*D*) mAb 10H10 does not immunoprecipitate a complex containing PDI. MPB-labeled cells were immunoprecipitated with mAb 9C3 or mAb 10H10 and probed for PDI, TF, or thiol biotinylation with MPB. (*E*) Dissociation of PDI from TF by bacitracin is reversible. (*F*) Bacitracin reversibly blocks TF·VIIa signaling. Wash out indicates that cells preincubated for 10 min with bacitracin were washed and equilibrated in serum-free medium for 10 min before stimulation with 10 nM VIIa. *, $P < 0.01$ relative to control (*t* test; mean ± SD; $n > 4$).

blocker PAO prevented inactivation of TF, indicating involvement of PDI to break the TF disulfide. NO reacts with GSH to yield GSNO, and the addition of GSNO was sufficient to suppress TF coagulant activity. A detailed biochemical analysis will be required to define which thiols in TF are susceptible to S-nitrosylation and whether the breakdown of GSNO yields glutathionation as an alternative modification of TF as well.

Complex Formation with PAR2 Is Required for TF·VIIa Signaling. mAb 5G9 had no effect on TF·VIIa signaling, but it showed strong reactivity with coagulant and noncoagulant pools of TF. This antibody immunoprecipitated a complex of TF with PAR2 from HaCaT cells (Fig. 5*A*). Hg^{2+} treatment to release surface PDI from TF abolished PAR2 complex formation with TF in mAb 5G9 immunoprecipitates. Pretreatment of cells with mAb 5G9 had no effect on the reverse association of TF with PAR2 immunoprecipitates, but the signaling blocking mAb 10H10 significantly reduced TF–PAR2 association (Fig. 5*B*). Thus, antibody blockade of TF·VIIa signaling was correlated with reduced TF·PAR2 coimmunoprecipitation. Unlike mAb 5G9, mAb 10H10 did not immunoprecipitate PAR2 (Fig. 5*C*) or PDI (Fig. 5*D*), indicating that this antibody prevents the formation of a complex involving TF, PAR2, and PDI.

Complete knockdown of PDI by siRNA was not achievable. We therefore inhibited PDI with bacitracin which, at 2–3 mM, is widely used to block cell-surface PDI function (25). Bacitracin was repurified to eliminate known enzymatic contaminants (26). To evaluate the effect of bacitracin on TF–PDI association, HaCaT cells were treated for 10 min with bacitracin followed by MPB labeling and TF immunoprecipitation with mAb 9C3. Bacitracin significantly reduced TF-associated PDI detected by Western blotting or MPB labeling (Fig. 5*E*). Cells were pretreated with bacitracin but then placed for an additional 10 min in serum-free medium. PDI reassociated with TF under this scheme. In the presence of bacitracin, TF·VIIa signaling was inhibited, but bacitracin did not block direct PAR2 agonist or thrombin signaling, demonstrating specificity (Fig. 5*F*). Washout experiments that resulted in PDI reassociation with TF (Fig. 5*E*) completely reversed the inhibitory effect of bacitracin on TF·VIIa signaling. Taken together, these data show in a cellular model with physiological levels of TF and PAR2 that PDI acts as a regulatory switch between direct TF·VIIa cell signaling and coagulation activation.

Discussion

The present data provide insight into the regulation of TF function on cells. By mutation, we show that the extracellular Cys^{186}–Cys^{209} disulfide bond is required for coagulation-activation as well as coagulation-initiation phase signaling by Xa in the ternary TF·VIIa·Xa complex but not for direct PAR2 cleavage by the binary TF·VIIa complex. Mutational breaking of this disulfide recapitulates the functional properties of the TF·VIIa signaling pool, which has low affinity for VIIa on cells with constitutive TF expression. We further demonstrate that TF coagulant activity is suppressed during association of extracellular PDI with TF and that disulfide/thiol-exchange pathways are required for TF·PAR2 complex formation and TF·VIIa signaling. These data delineate the biochemical mechanism by which TF·VIIa is switched from coagulation to direct cell signaling and thus provide a solution to the fundamental problem of how TF·VIIa signaling can occur independently of coagulation activation.

Our study adds an unexpected aspect to the biology of extracellular disulfide-exchange pathways by demonstrating versatility to switch a single receptor between two distinct biological activities. Disulfide/thiol exchange is an allosteric mechanism to control extracellular proteolysis, matrix remodeling, and cell adhesion, and S-nitrosylation has been demonstrated to regulate integrin activation (27–32). The presented data indicate that breaking of the Cys^{186}–Cys^{209} disulfide bond to inhibit TF coagulant function is similarly under the control of NO pathways. Vascular-protective NO synthesis is frequently perturbed in atherosclerosis, diabetes, or inflammation (33), and uncoupling of NO synthesis may shift cell-surface TF activity to coagulation. NO-dependent inhibition of TF coagulant activity thus links the regulation of thrombogenicity in an unexpected way to oxidative stress in cardiovascular disease and inflammation.

The biochemical evidence for a switch in TF functional specificity is further corroborated by conformational changes detected by mAb 10H10. mAb 10H10 has low affinity for coagulant TF, but it binds the noncoagulant, cryptic pool of TF efficiently. mAb 10H10 either prevents formation or actually disrupts the TF·PAR2 complex and thus inhibits TF·VIIa signaling. This finding implies the existence of a pool of signaling TF that is distinct from other noncoagulant pools. From the low expression levels of monomeric C209A TF we deduce that a small fraction of TF is sufficient for TF·VIIa signaling, but at present there is no antibody that reacts selectively with the complex of TF with PAR2 without recognizing other pools. PDI and thiol pathways are critical for TF·VIIa signaling, and we found a close correlation between TF–PDI association and TF·VIIa signaling in several cell types, including breast cancer cells. Preliminary experiments further demonstrate that blockade of TF·VIIa signaling in these cells by mAb 10H10 is superior to blocking coagulation by mAb 5G9 to suppress tumor growth, emphasizing the relevance of the TF·VIIa signaling pathway *in vivo*. Importantly, mAb 10H10 has minimal effects on coagulation activation, providing initial evidence that inhibition of TF·VIIa signaling is feasible without impairing hemostasis.

Methods

Reagents. Coagulation factors, inhibitors, and antibodies were described previously (4, 8, 12, 34), or they were obtained from the following suppliers: anti-PDI RL90 and SNP from Alexis (Carlsbad, CA); anti-ERP57 from Upstate (Lake Placid, NY); MPB from Molecular Probes (Eugene, OR); GSNO from Cayman (Ann Arbor, MI); NHS-biotin from Pierce (Rockford, IL); and ascorbic acid, bacitracin, and PAO from Sigma (St. Louis, MO). Bacitracin was repurified by gel filtration and tested for the absence of enzymatic activity that degrades PDI (26). Rabbit anti-PAR2 was raised against TIQGTNRSSKGRSLIGKVDGTSHVTGCG thiol coupled to keyhole limpet hemocyanin. His-tagged soluble TF mutants were expressed in *Escherichia coli*, as described in ref. 35.

Cell Culture. HUVECs were maintained and transduced as described in ref. 8. Human HaCaT keratinocyte standard culture medium contained DMEM, 10% (wt/vol) FBS, and 2 mM glutamine. To analyze TF expression under growth arrest, cells in logarithmic growth were replated at high density and followed over time. For low-Ca^{2+} culture, cells were split into keratinocyte-SFM (Invitrogen, Carlsbad, CA) and 10% (vol/vol) calcium-depleted FBS for 48 h and switched by adding 2 mM Ca^{2+} for 24 h. For siRNA knockdown, HaCaT cells were transfected daily at 40% confluence with 100 nM siRNA (Santa Cruz Biotechnology, Santa Cruz, CA) by using 2 μl of Lipofectamine 2000 (Invitrogen).

Functional and Signaling Assays. Cells were equilibrated to serum-free conditions in medium 199 (Irvine Scientific, Santa Ana, CA)/2 mM glutamine/10 mM Hepes, pH 7.4/1.5 mM Ca^{2+} for 5 h (HUVECs) or in DMEM/2 mM glutamine/10 mM Hepes, pH 7.4, for 10 min (HaCaT cells). Inhibitors were added 10 min before stimulation at the following concentrations: anti-TF (50 μg/ml), rabbit anti-PAR2 (100 μg/ml), anti-PAR1 (ATAP2, 20 μg/ml, WEDE15, 40 μg/ml), and bacitracin (3 mM). Hirudin (200 nM) was added routinely to exclude thrombin signaling. MAP kinase phosphorylation after 10 min of agonist stimulation was quantified by Western blotting (20).

Cell-Surface Labeling, Immunoprecipitation, and Confocal Imaging. Cells were washed and pretreated with thiol blockers where indicated in Hepes buffer, pH 7.4, with 1.5 mM Ca^{2+} for 15 min at ambient temperature. After washes with the same buffer, cells were labeled with either 100 μM MPB or 0.5 mg/ml NHS-biotin in the presence or absence of 1 mM ascorbic acid at 4°C for 20 min. After quenching amino labeling with Tris and extensive washing, immunoprecipitations from 50 mM *n*-octyl β-D-glucopyranoside lysates used mAbs directly coupled to Dynabeads (Invitrogen). Western blotting was performed with affinity-purified goat anti-TF, anti-PDI RL90, or streptavidin-conjugated horseradish peroxidase for biotin detection. Blots were digitized for densitometry by using Scion Image (Scion, Frederick, MD). Cells were stained on ice with directly conjugated antibodies for confocal microscopy using a Nikon TE2000-U microscope (Nikon Instruments, Melville, NY). Optical sections of each fluorophore were merged by using Photoshop (Adobe, San Jose, CA).

We thank Pablito Tejada, Jennifer Royce, Cindi Biazak, Rachael Kamps, and David Revak for assistance and Barbara Parker for figure preparation. This work was supported by National Heart, Lung, and Blood Institute/National Institutes of Health Grant HL31950 (to W.R.), American Heart Association Grant 04250024 (to J.A.), and Netherlands Scientific Organization Grant S92-251 (to H.H.V.).

1. Norledge B, Petrovan RJ, Ruf W, Olson A (2003) *Proteins* 53:640–648.
2. Mackman N (2004) *Arterioscler Thromb Vasc Biol* 24:1015–1022.
3. Camerer E, Huang W, Coughlin SR (2000) *Proc Natl Acad Sci USA* 97:5255–5260.
4. Riewald M, Ruf W (2001) *Proc Natl Acad Sci USA* 98:7742–7747.
5. Riewald M, Ruf W (2003) *Crit Care* 7:123–129.
6. Belting M, Ahamed J, Ruf W (2005) *Arterioscler Thromb Vasc Biol* 25:1545–1550.
7. Ossovskaya VS, Bunnett NW (2004) *Physiol Rev* 84:579–621.
8. Ahamed J, Ruf W (2004) *J Biol Chem* 279:23038–23044.
9. Belting M, Dorrell MI, Sandgren S, Aguilar E, Ahamed J, Dorfleutner A, Carmeliet P, Mueller BM, Friedlander M, Ruf W (2004) *Nat Med* 10:502–509.
10. Bach RR (2006) *Arterioscler Thromb Vasc Biol* 26:456–461.
11. Rao LV, Pendurthi UR (2005) *Arterioscler Thromb Vasc Biol* 25:47–56.
12. Ruf W, Rehemtulla A, Edgington TS (1991) *Biochem J* 278:729–733.
13. Huang M, Syed R, Stura EA, Stone MJ, Stefanko RS, Ruf W, Edgington TS, Wilson IA (1998) *J Mol Biol* 275:873–894.
14. Le DT, Rapaport SI, Rao LVM (1992) *J Biol Chem* 267:15447–15454.
15. Hjortoe GM, Petersen LC, Albrektsen T, Sorensen BB, Norby PL, Mandal SK, Pendurthi UR, Rao LV (2004) *Blood* 103:3029–3037.
16. Rehemtulla A, Ruf W, Edgington TS (1991) *J Biol Chem* 266:10294–10299.
17. Hogg PJ (2003) *Trends Biochem Sci* 28:210–214.
18. Wouters MA, Lau KK, Hogg PJ (2004) *BioEssays* 26:73–79.
19. Schmidt B, Ho L, Hogg PJ (2006) *Biochemistry* 45:7429–7433.
20. Ahamed J, Belting M, Ruf W (2005) *Blood* 105:2384–2391.
21. Zai A, Rudd MA, Scribner AW, Loscalzo J (1999) *J Clin Invest* 103:393–399.
22. Ramachandran N, Root P, Jiang XM, Hogg PJ, Mutus B (2001) *Proc Natl Acad Sci USA* 98:9539–9544.
23. Sliskovic I, Raturi A, Mutus B (2005) *J Biol Chem* 280:8733–8741.
24. Jaffrey SR, Erdjument-Bromage H, Ferris CD, Tempst P, Snyder SH (2001) *Nat Cell Biol* 3:193–197.
25. Mandel R, Ryser HJ, Ghani F, Wu M, Peak D (1993) *Proc Natl Acad Sci USA* 90:4112–4116.
26. Rogelj S, Reiter KJ, Kesner L, Li M, Essex D (2000) *Biochem Biophys Res Commun* 273:829–832.
27. Pimanda JE, Annis DS, Raftery M, Mosher DF, Chesterman CN, Hogg PJ (2002) *Blood* 100:2832–2838.
28. Stathakis P, Fitzgerald M, Matthias LJ, Chesterman CN, Hogg PJ (1997) *J Biol Chem* 272:20641–20645.
29. Essex DW, Li M, Miller A, Feinman RD (2001) *Biochemistry* 40:6070–6075.
30. Lahav J, Wijnen EM, Hess O, Hamaia SW, Griffiths D, Makris M, Knight CG, Essex DW, Farndale RW (2003) *Blood* 102:2085–2092.
31. Walsh GM, Sheehan D, Kinsella A, Moran N, O'Neill S (2004) *Biochemistry* 43:473–480.
32. Root P, Sliskovic I, Mutus B (2004) *Biochem J* 382:575–580.
33. Dudzinski DM, Igarashi J, Greif D, Michel TM (2005) *Annu Rev Pharmacol Toxicol* 46:235–276.
34. Dorfleutner A, Hintermann E, Tarui T, Takada Y, Ruf W (2004) *Mol Biol Cell* 15:4416–4425.
35. Stone MJ, Ruf W, Miles DJ, Edgington TS, Wright PE (1995) *Biochem J* 310:605–614.